

Progress in the Assessment of Complex Components

ERWIN SOMMER

*Fraunhofer-Institut für Werkstoffmechanik, Wöhlerstr. 11,
7800 Freiburg, FRG*

1. INTRODUCTION

One of the important aims of fracture mechanics is the development of methods for assessing the integrity of components and structures. Unfortunately the complexity of the problem allows only partial solutions taking into account the variety of structures due to their differences in material properties, loading as environmental conditions and geometrical design. From experience is known that failure is most likely initiated at defects, inclusions, flaws, cracks. Therefore, most of the procedures concentrate on the investigation of structures containing real or postulated defects or cracks.

Since investigations of full-size structures are time-consuming and expensive the basic idea is to simulate the most severe features of the material conditions and the loading situations of complex components in specimens which are easier to handle under laboratory conditions, and to use the results obtained in order to quantify the margin of safety of the components, their availability or their remaining lifetime by extrapolation.

The main concern is how to abstract a "typical" material condition or loading situation of a component and to model it in a specific specimen configuration since a multitude of parameters can be of importance for the final failure. In general the spectrum of parameters is so wide that the transferability of results from specimens to components can only be guaranteed for a limited range of application. Therefore only solutions will be obtained whose range of validity strictly has to be observed. The more general a solution is, the less representative it may describe a specific situation in a structure.

One of the most suitable methods developed for assessing components containing known or postulated defects is the R6 procedure for constructing a failure assessment diagram. This procedure specifies the limiting condition of a structure by

reference to the two principal criteria: fracture or plastic collapse. Depending on the purpose of the analysis and the availability of test data three different categories of assessment procedures with increasing resolution can be selected to evaluate (Milne et al., 1986)

- the limiting load to avoid failure of a structure
- the limiting crack size of the structure subjected to a specific loading condition
- the reserve factors on the assessed conditions
- the sensitivity of these reserve factors to the assessed conditions and details of the analysis.

The R6 procedure embraces a worldwide experience in fracture mechanics and covers a wide range of application.

Nevertheless there are still remaining assessment problems of practical interest which are concerned with the investigation of situations or parameter variations excluded in the R6 procedure or covered in a generalizing manner.

According to the R6 procedure the integrity of a structure for example is evaluated with reference to an existing or postulated flaw, a single load application below the creep range and a material-specific resistance against failure. When changes of the size or the shape of the defect due to stable or subcritical flaw growth by mechanisms such as ductile tearing, fatigue and environmentally assisted crack growth are to be expected they independently have to be accounted for. Furthermore in many cases not only the onset of failure, but the complete failure process has to be assessed. "Leak before break" considerations may stand as a typical example.

For further refinement of assessment procedures the following discussion will concentrate on some investigations of this kind as

- The growth characteristics of cracks extending in components of ductile behavior. These characteristics are important for a precise description of the complete failure process or a prediction of the remaining lifetime as well as for the assessment whether initial defects will change in size or shape.

This includes the discussion of three-dimensional effects such as parameter variations which influence

- the local loading parameters along the contour of cracks as well as
- the local fracture resistance.

Complete other areas as the progress in the assessment of fracture by fatigue, creep or corrosion will be excluded in this discussion.

2

GROWTH CHARACTERISTICS OF CRACKS

In order to provide information on a stable or subcritical extension of a defect to be assessed or even on the probable crack path and the future shape of a crack front the growth behavior of cracks has to be investigated. Due to the number of

variables involved analytical predictions are in general extremely difficult.

Since one of the most dangerous defect configuration is given by a crack under the mode I loading and since due to manufacturing, handling and service defects at the surface of structures are most likely to exist many investigations have been devoted to surface crack problems.

According to the principles of fracture mechanics it is expected that at any given position of a crack front fracture should initiate and extend where the locally released energy exceeds the fracture resistance of the material. In cases where the local loading situation as well as the resistance are varying usually in a simplifying manner an assessment is based on the comparison of the maximum of the loading parameter with the minimum of the resistance. Since this value is unknown for the real defect situation in the structure it is replaced by the lowest resistance value obtained in specimens under the most severe constraint situation. This procedure guarantees a safe but not a representative answer, i.e. the answer may be too conservative.

For a more precise evaluation the distribution of the loading parameters and the fracture resistance along the contour of the crack to be assessed have to be known. Depending upon the mechanisms of failure to be expected the first part of the problem without too great difficulties can be solved by computing the variation of the stress intensity factor $K(s)$, the strain energy release rate $G(s)$ governing the elastic regime or $J(s)$ in the elastic-plastic regime. A variety of suitable solutions especially for surface crack configurations under remote tension or bending in plates or pipes are available in the literature, (e.g. Newman, 1979, Swedlow, 1972, McGowan, 1980, Schmitt, 1986, Brocks and Noack, 1987). The second part of the problem, the determination of the local fracture resistance at the contour is even more challenging. The local resistance only experimentally can be obtained. Since precise methods for the determination are lacking for the sake of simplicity a constant resistance often is assumed. As such a simplified example the loading situation in a surface crack with a constant resistance is considered in Fig. 1 (Sommer, 1984). This consideration in principle refers to the initiation and beginning growth of the crack in a stable or unstable manner. The same consideration will apply for subcritical growth of cracks by fatigue or environmentally assisted. That the assumption of a constant resistance along the contour becomes doubtful the more plastic deformation at the crack tip occurs simply can be demonstrated by the changes in the shape of cracks propagated by fatigue with increasing load steps (Hodulak et al., 1978, 1977a) (Fig. 2). From experimental investigations it is known that in some cases the maximum of crack growth does not correspond to the maximum of the loading parameter. The "canoeing" effect observed for cracks propagating in a ductile manner (Sommer et al., 1977, Brocks et al., 1988) (Fig. 3) e.g. cannot be explained by relying on the loading parameter only. Agreement can be obtained when in

addition a variation of the local fracture resistance is assumed.

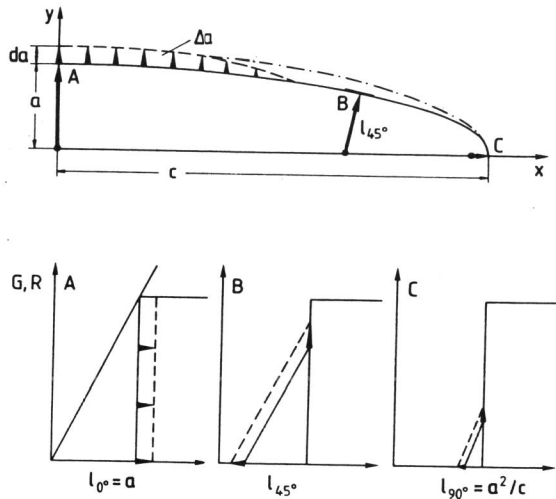


Fig. 1. Local Fracture Initiation of a Surface Crack ($a/c = a/t = 0.2$) in a Plate under Tension; Brittle Material Behavior; Constant Fracture Resistance Along the Contour.

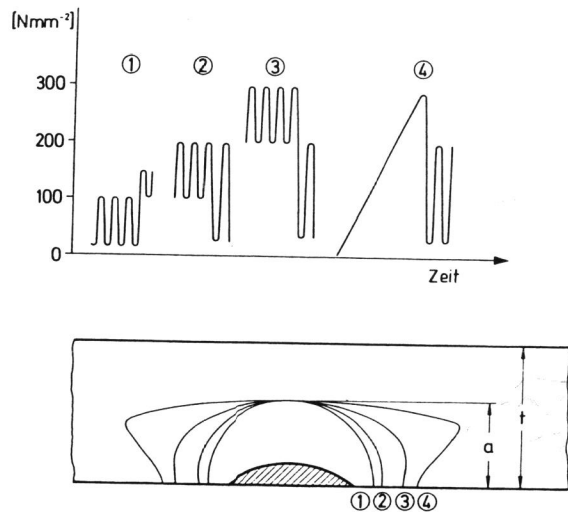


Fig. 2. Resulting Crack Shapes for $a/t = 0.6$ Under Various Loading Conditions.

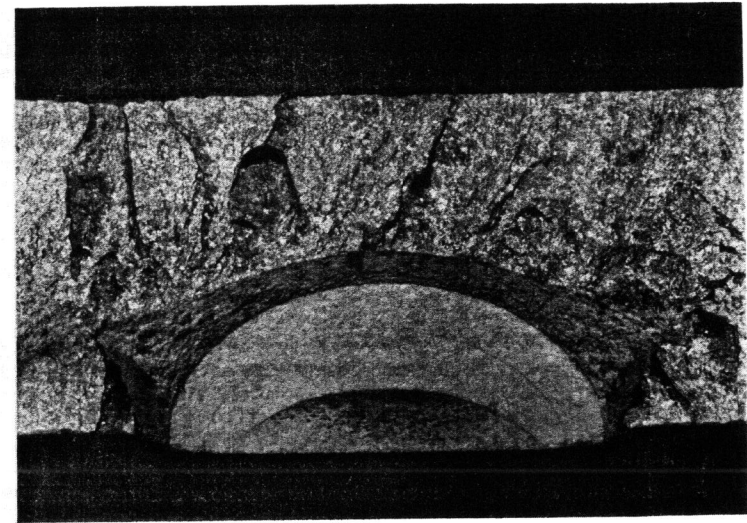


Fig. 3. Fracture Surface in a Prefatigued Plate of 22 NiMoCr 3 7 under Uniform Tension Showing Canoeing Effect.

For the explanation of three-dimensional effects a careful interpretation of results obtained under simplifying "two-dimensional" or plane conditions is helpful.

2.1. Observations in Plane Specimens

From fracture test results carried out in plane specimens of the same material it is known that the onset and growth of fracture is strongly affected by the temperature, the strain rate and the prevailing stress state. In such plane specimen configurations which contain cracks with a more or less straight front - in contrast to the surface crack problem - usually the loading and the resistance parameters are tacitly defined as mean values averaged in the thickness direction (s. section "Correlation of Fracture Resistance and Multiaxiality"). This allows to suppress a discussion on their possible variation along the contour. Correspondingly information on the stress state is only available in an averaged form. The importance of this fact will be stressed in the following discussion.

Since the state of plane strain is considered as the most dangerous one - as a well known consequence - care is taken by restricting the design of specimens for the determination of fracture toughness values as K_{Ic} or J_{Ic} in such a way that in the near field of the crack tip this stress state dominates (ASTM Standards, 1969, ASTM E 813-82).

The slope of fracture resistance curves as J_R versus Δa is even more affected by the global and local constraint of the specimen. Sidegrooved compact specimens of sufficient thickness provide the most severe constraint conditions leading to resistance curves of the lowest slope. This effect is pronounced in materials with ductile behavior as metals. Materials with brittle behavior as ceramics which allow to construct resistance curves sometimes also show a great variation in the slope. These changes in slope, however, are mainly dominated by other effects as the crack path dependent fracture mechanisms in the process zone.

2.1.1. Fracture Initiation and Resistance

For a refined interpretation of these effects based on a distinct separation of the parameter of main influence reproducible experimental results with a limited scatter have to be available.

The onset of brittle fracture of specimens under monotonically increasing, but quasistatic loading can be characterized in the well known relatively simple manner using instability criteria based on LEFM-methods by critical values of the parameters - stress intensity factor K or strain energy release rate G . However, the characterization of the initiation of fracture in the EPFM-regime in terms of the parameter J needs more effort.

2.1.1.1. Fracture Initiation and Resistance in Ductile Materials

For the characterization of the initiation toughness of ductile materials the following evaluation procedures are often used (Blauel et al. 1984)

J_{IC}^{ASTM} : technical initiation toughness - evaluated from a

linear fit to the J_R -curve according to ASTM E 813-81

J_{IC}^{Loss} : technical initiation toughness - evaluated from a power law fit according to (Loss et al. (1979)

J_i : physical initiation toughness - estimated as the first point of deviation of the J_R -curve from the formal blunting line.

As an example the toughness of the reactor pressure vessel steel 20 MnMoNi 55 determined according to the several evaluation procedures in Fig. 4 are plotted versus temperature. Within the pronounced scatterband of the results these J_i -values seem to be independent of geometry parameters - at least in the range of variation of CT 25 to CT 100 with and without sidegrooves - and of temperature - in the range of

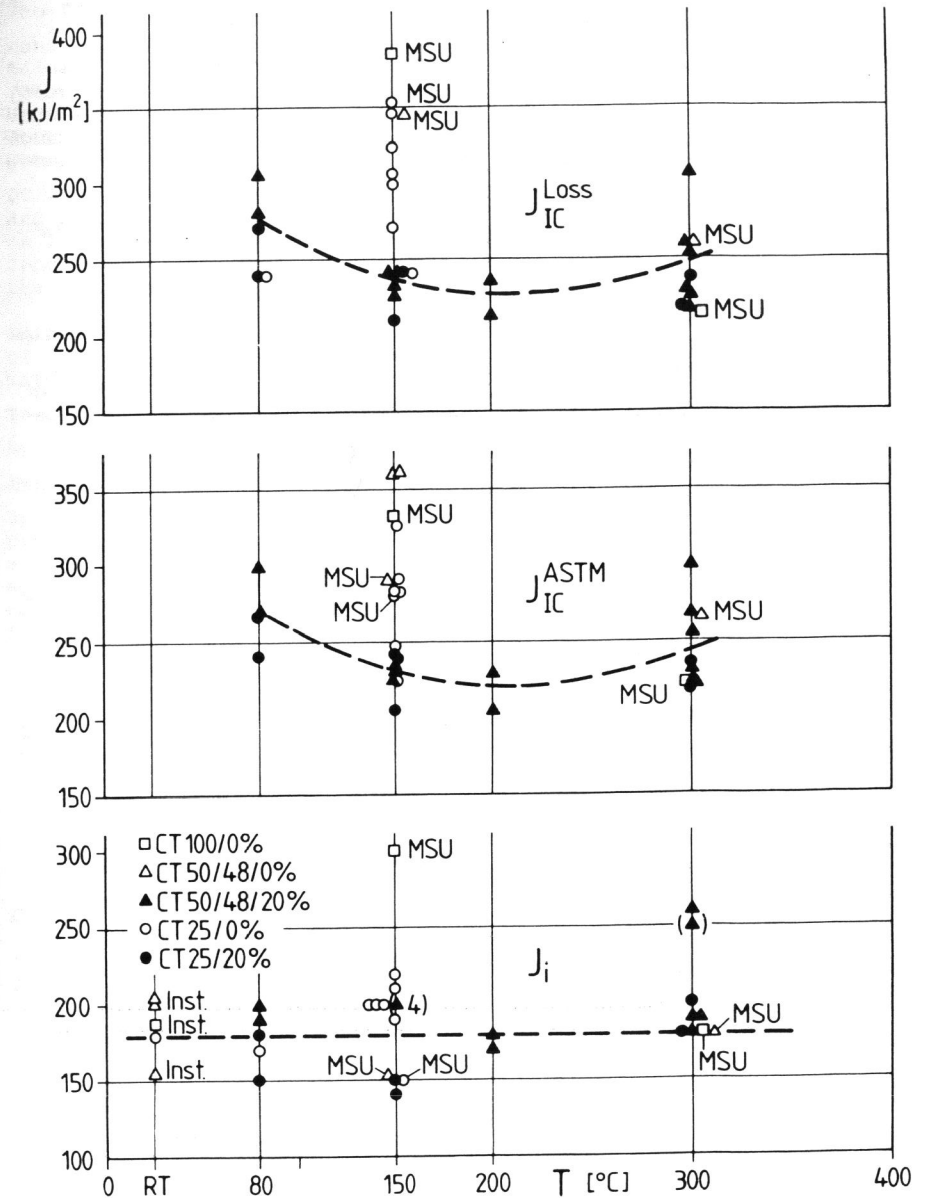


Fig. 4. Initiation Toughness as a Function of Temperature ; Pressure Vessel Steel 20 MnMoNi 55. (Blauel et al. 1984.)

variation RT to 300°C -. The resulting mean value is $J_i^{\text{mean}} = 180 \text{ N/mm}$.

The "technical" toughness values do not describe the real initiation of fracture. They are determined after a finite amount of stable crack growth occurred and are accordingly higher than the physical initiation toughness values. In addition temperature trends can be observed at about 200°C.

These experimental results are confirmed for different steels by the findings of other authors (Roos et al., 1987).

Since J_i -values of this kind are determined from the first change in the slope of J_R -curves it has to be recalled that the J -evaluation is a procedure averaging over the thickness and in addition is related to the net section of the ligament when specimens with and without sidegrooves are considered. The experimental error of about 10 to 20 % in general obscures a more precise interpretation of these test results. Trends which allow an even more refined assessment can be observed and will be discussed in section "Correlation of Fracture Resistance and Multiaxiality".

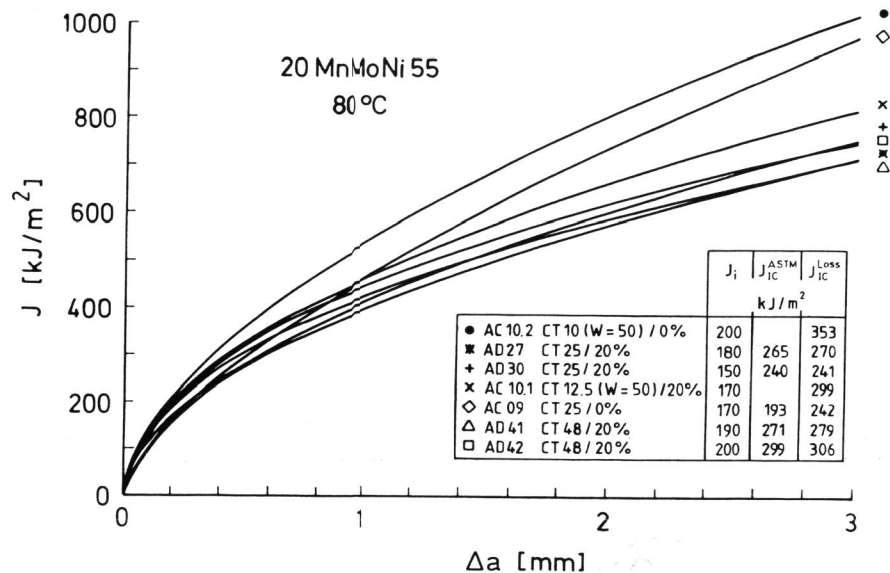


Fig. 5. J_R -Curves and Critical J_i -Values Obtained from Different CT-Specimens at 80°C with the Partial Unloading Technique for the Reactor Pressure Vessel Steel 20 MnMoNi 55. (Blauel et al. 1984.)

The influence of the specimen geometry on J_R -curves due to constraint effects is demonstrated in Fig. 5 by results obtained for the reactor vessel steel 20 MnMoNi 55 at 80°C (Blauel et al., 1984) which may stand for similar results of other authors (Roos et al., 1987). Seven CT-specimens ranging from 10 to 48 with and without sidegrooving have been investigated. The resulting slope of the J_R -curves is steepest for the CT (0 % s.g.) 10 and 25 and lowest for the CT (20 % s.g.) 48 and 25; the slope of the CT (20 % s.g.) 12.5 specimen is almost as low as for the CT (20 % s.g.) 25 and 48 which leads to the conclusion that the 20 % sidegrooving has a stronger effect on the slope than doubling the specimen thickness.

In order to establish quantitative results on the reliability of tests which allow to distinguish between experimental and material scatter of J_R -curves the European Group on Fracture, Task Group I, carried out round robin investigations supported by 13 laboratories (Blauel and Voss, 1986). J_R -curves are analyzed by various techniques according to the position of the specimens in one of three layers across the thickness of a plate of the steel A 542. As demonstrated in Fig. 6 the scatter within each subset is less than the total scatterband. The specimens taken from the center layer of the plate have a lower resistance compared to the specimens taken from the near surface. In conclusion of these results it can be stated that the

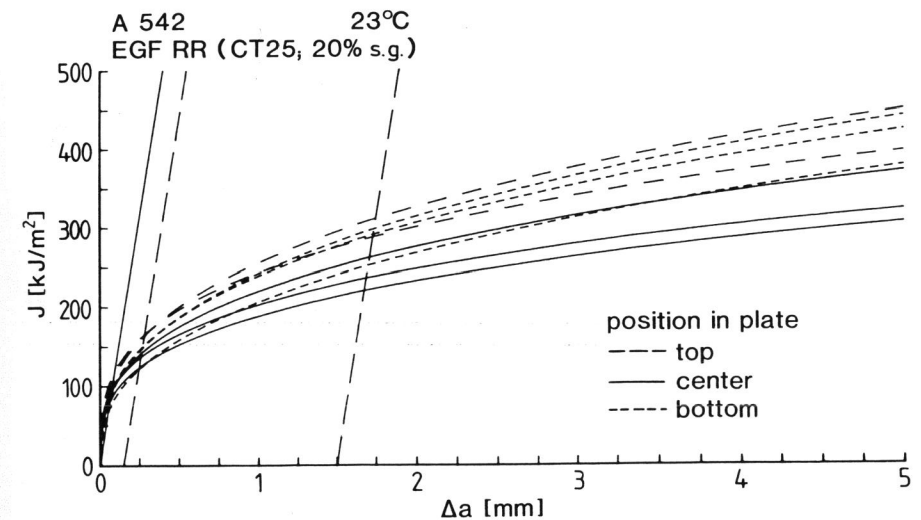


Fig. 6. J_R -Curves Obtained by Regression $J = C \Delta a^n$ for Sidegrooved CT 25 Specimens Investigated by 13 Different Laboratories (EGF Round Robin) at 23°C; Steel A 542. (Blauel and Voss, 1986.)

high standard of the single specimen method allows to resolve the different sources of scatter and therefore to attack the problem of the influence of the geometry i.e. mainly the influence of constraint on the slope of J_R -curves.

2.1.2. Multiaxiality Parameter

The constraint is considered to be the restraint of plastic deformation due to the complete stress state in the specimen. Quantitatively the term constraint is difficult to define. For ductile fracture the multiaxiality parameter

$\sigma_m / \sigma_v = h(r, \varphi, s)$ successfully has been applied

to characterize the local constraint at the crack tip (Claussmeyer, 1969, Roos et al., 1986, BAM-Forschungsbericht, 1987)

where

$\sigma_m = (\sigma_1 + \sigma_2 + \sigma_3) / 3 = \text{mean stress and}$

$$\sigma_v = 2^{-1/2} [(\sigma_1 - \sigma_2)^2 + (\sigma_3 - \sigma_1)^2 + (\sigma_2 - \sigma_3)^2]^{1/2} = \text{equivalent stress}$$

evaluated in dependence on the crack tip coordinates r, φ, s . It is expected that the constraint represented by the function

$\sigma_m / \sigma_v = h(r, \varphi = 0, s)$ on the ligament is most important for mode I fracture. Therefore only the function $\sigma_m / \sigma_v = h(r, s)$ is investigated on the ligament along the contour of cracks i.e. in dependence of the parameter s at a certain distance r from the crack tip.

The importance of this parameter will be demonstrated by numerical calculations which simulate experimentally investigated CT 20 specimens of the reactor pressure vessel steel 22 NiMoCr 3 7 at RT. The resulting J_R -curves are plotted in

Fig. 7; two of the curves with a higher resolution in Fig. 8. The stress-strain-curve of the material is assumed to be a multilinear curve, the $1/r$ -singularity of the crack tip strain by collapsed isoparametric elements. The radius of curvature of the sidegrooves is modelled by $\rho = 0.25$ mm improving the results reported in (Kordisch and Sommer, 1986).

The variation of J along the crack contour for both specimen configurations is computed by the virtual crack extension method using IWM-Crack (IWM-CRACK, 1988) and plotted in Figs. 9 a and b for several load steps. For the CT-specimen without sidegrooves the ratio $J_{\text{center}} / J_{\text{surface}}$ increases with increasing load. For the CT-specimen with sidegrooves J is relatively constant and decreases only slightly towards the free surface.

Figs. 10 a and b show the corresponding variation of the factor of multiaxiality σ_m / σ_v along the crack contour evaluated on the

ligament at a distance 0.24 mm from the crack tip. With increasing displacement σ_m / σ_v approaches a limiting value in the center of both specimens of $(\sigma_m / \sigma_v)_1 = 2.8$. When $\sigma_m / \sigma_v = h(r, s)$ is calculated by FE-methods the accuracy of the results obtained depends on the technique used for modelling the crack tip field, the type and mesh size of the elements (Brocks and Noack, 1987, Kordisch et al., 1987). Most commonly used is the collapsed element technique which allows modelling of e.g. $1/r$ -singularities in the strains and non-zero crack tip displacements. If no geometric non-linearities are considered (material non-linear only MNLO-option in ADINA, (Bathe, 1980) the element stiffness matrices built are based on the original undisplaced position of the nodal points and thus this singular behavior is maintained throughout the analysis for all load steps. In such an analysis the stress components evaluated at the integration points increase towards the crack tip according to the singular behavior of the strains and to the non-linear material description. If in addition also geometric non-linearities are taken into account (e.g. the updated Lagrangian UL-option in ADINA) and a fine mesh size is used the computed function $\sigma_m / \sigma_v = h(r)$ shows a maximum at a definite distance from the crack tip. For the same material properties and the same J -level this maximum is mainly affected by the effects related to the specimen geometry (BAM-Forschungsbericht, 1987; Brocks et al., 1987) (Fig. 11). For scanning purposes the calculation under the assumption of non-linear material behavior

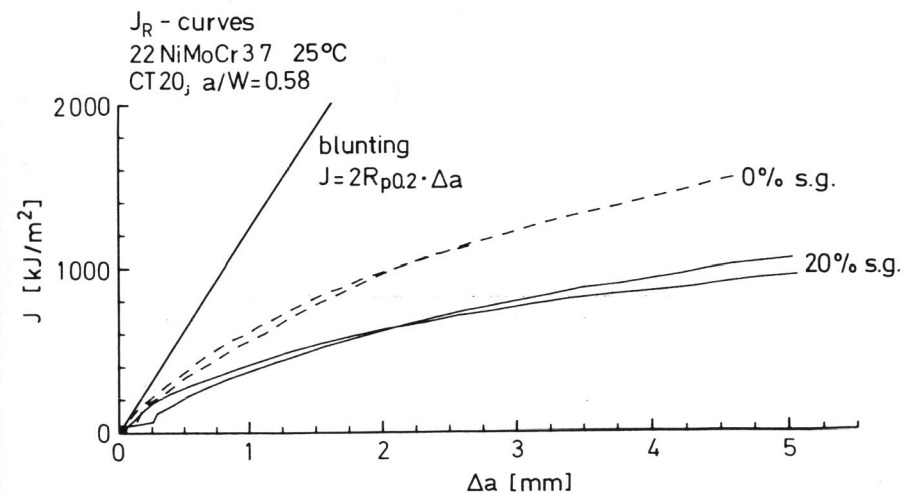
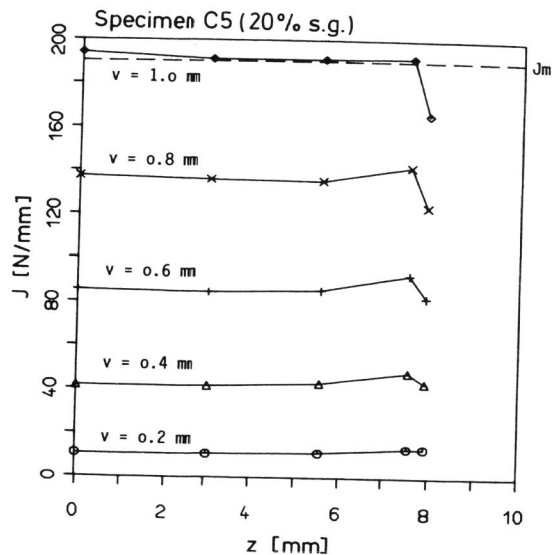
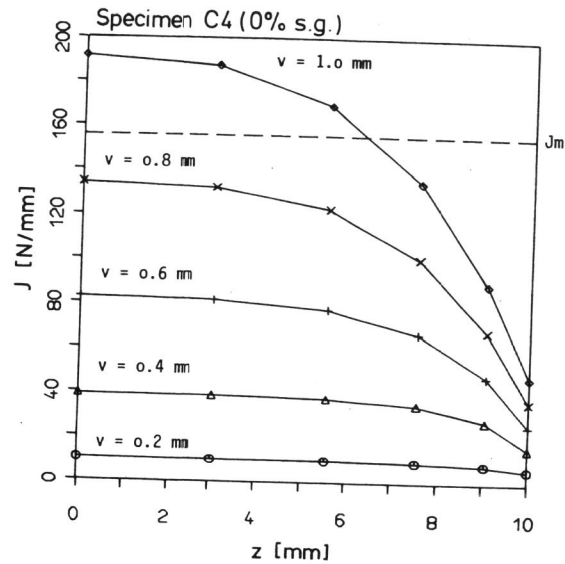


Fig. 7. J_R -Curves at CT 20 Specimens 0 % and 20 % Sidegrooved; Reactor Pressure Vessel Steel. (Kordisch et al., 1987).



Figs. 9 a and b. J Along the Crack Front of Compact-Specimens with (20 %) and without Sidegrooving.

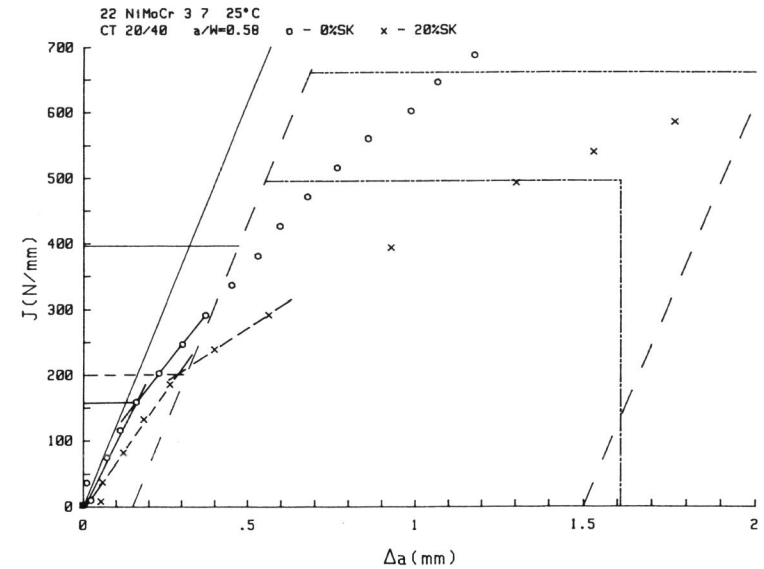


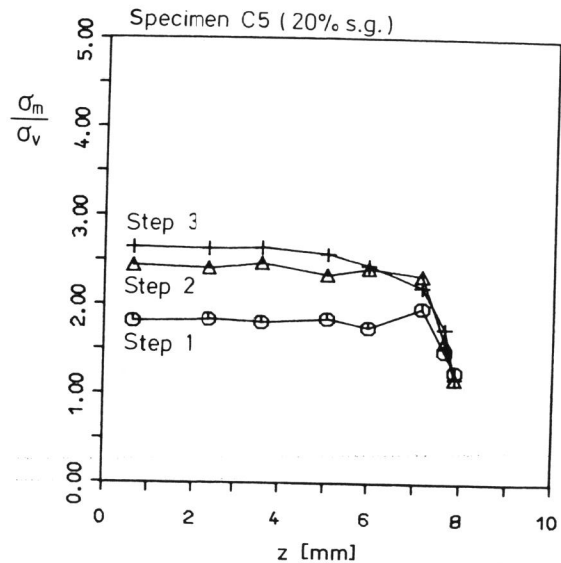
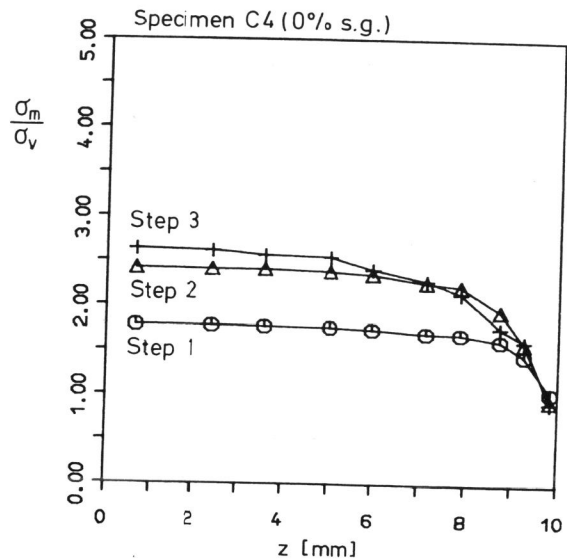
Fig. 8. Details of Fig. 7; Two Curves Selected from Four in Order to Demonstrate the Difference in the Onset of Stable Crack Growth for Specimens 0 % and 20 % s.g.

only (MNLO) as a kind of integrating approach applied in (Schmitt, 1986; Kordisch and Sommer, 1986). In the case of MNLO an extrapolation to the crack tip ($r = 0$) leads to limiting values which correspond roughly to the maximum values obtained by the other modelling technique. The calculation reported in Figs. 7 and 8 have been based on the MNLO modelling technique (Kordisch et al., 1987).

2.1.3. Correlation of Fracture Resistance and Multiaxiality

Both specimen configurations show for the same step of external displacement in the center the same value of the loading parameter J as well as the limiting value of the parameter $(\sigma_m / \sigma_v)^2$.

When fracture is assumed to be initiated as a local event at a definite $J_{initiation}$ -value fracture in both cases should start at the same central J-value inspite of the differences in the J-distribution caused by the specimen geometry. That this hypothesis is in agreement with experimental findings can be indirectly proved. The two single J_R -curves plotted in Fig. 8 which are obtained from a CT-specimen with (20 %) and without (0 %) sidegrooving.



Figs. 10 a and b. Parameter of Multiaxiality σ_m / σ_v Along the Crack Front of the Same Specimens.

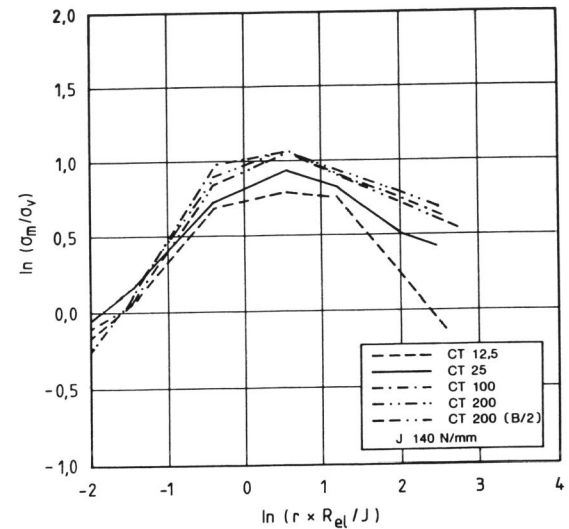


Fig. 11. Parameter of Multiaxiality σ_m / σ_v in Compact-Specimens Versus the Normalized Ligament Coordinate in the Midsection of the Specimen. (Brocks et al. 1987.)

sidegrooving allow to determine fracture initiation values. These are the average values: J_{mi} (20 % s.g.) = 200 ± 20 N/mm and J_{mi} (0 % s.g.) = 160 ± 20 N/mm. The numerically calculated plots of the J-distribution along the contour of the specimens with and without sidegrooves in Fig. 9a and b show that for the same local value $J_i = 190$ N/mm different average values J_{mi} of the same order as experimentally obtained results.

For the same step of external displacement the same local values in the center of the two specimen configurations result but different mean values J_m and $(\sigma_m / \sigma_v)_m$. They are defined as the weighted integral over the thickness B:

$$J_m = B^{-1} \int J(z) dz \quad \text{and} \quad (\sigma_m / \sigma_v)_m = B^{-1} \int (\sigma_m / \sigma_v)(z) dz$$

When fracture resistance curves - J_{exp} versus stable crack growth Δa - experimentally are determined J_{exp} has to be considered as the average value J_m . The parameter $(\sigma_m / \sigma_v)_m$ obtained at a certain distance from the crack tip for corresponding specimen geometries can help to explain the observed differences in the experimentally resulting slope $\Delta J / \Delta a$.

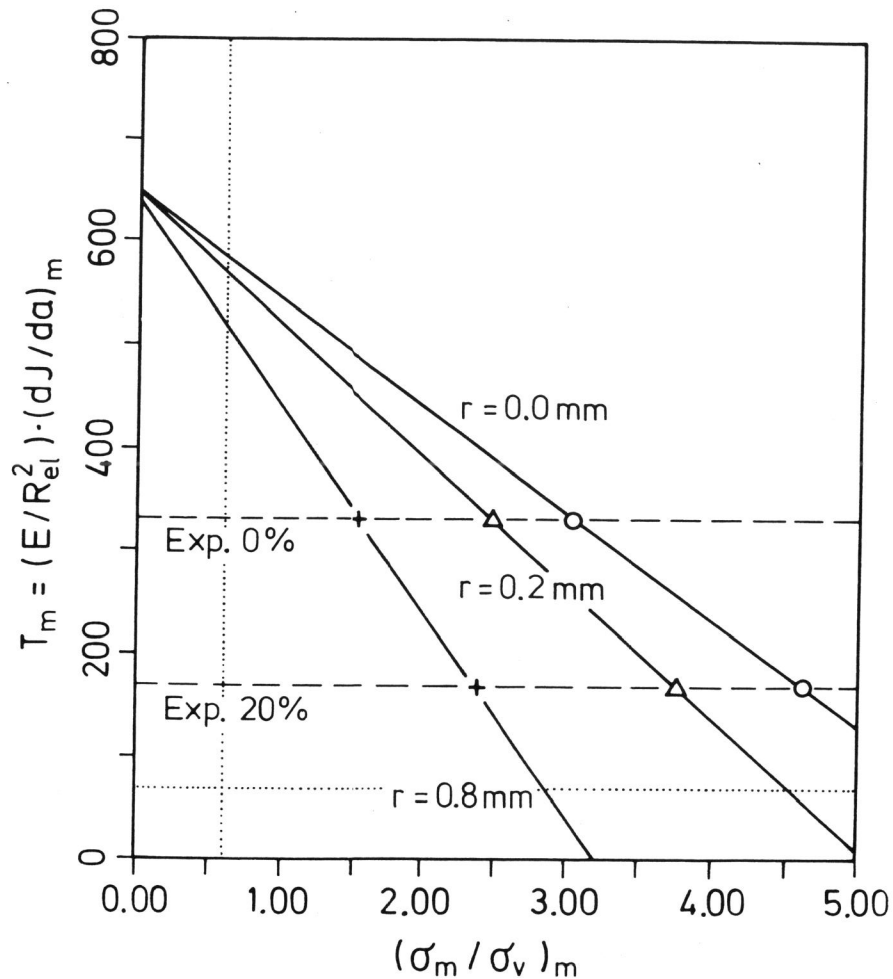


Fig. 12. Correlation of Slope $\Delta J/\Delta a$ with Mean Value $(\sigma_m / \sigma_v)_m$ for Different Crack Tip Distances r .

Therefore, in Fig. 12 the experimentally from Fig. 7 determined $\Delta J/\Delta a$ - values for the two types of specimens (0 % sidegrooved: $\Delta J/\Delta a \approx 490 \text{ N/mm}^2$; 20 % sidegrooved: $\Delta J/\Delta a \approx 250 \text{ N/mm}^2$) are plotted versus the corresponding $(\sigma_m / \sigma_v)_m$ -values calculated at different distances of the crack tip. As a first approximation a linear relationship is assumed and postulated by extrapolation for establishing the slope of resistance curves for cracks in components under different constraint situations.

2.2. Application to Complex Structures

As a first example the assessment of axial through-the-thickness cracks in a cylindrical vessel of 3 m length, 1.5 m diameter and 40 mm wall-thickness based on J_R -curves will be considered (Aurich et al., 1986). In Fig. 13 the resulting J_R -curve is compared with those of different plane specimens. The plot demonstrates that the J_R -curves obtained for the double edge cracked tension (DECT) and the compact tension (CT) specimens describe a more severe constraint situation expressed by the lowest slope than the axial cracks ($2a = 104$ to 450 mm) in the vessel whereas the center cracked tension (CCT) specimens show the lowest constraint.

The situation described may be considered as a first step in the chain of transferability of results from specimens to components. In a next step the extension of surface cracks in components will be discussed. Investigations of this kind have been carried out for example in (Kordisch and Sommer, 1986; Brocks et al., 1987; Brocks and Noah, 1987), the following results explained in this paper are cited from (Klemm et al., 1988).

Stable growth of a surface crack in a structure can be predicted when the local distribution of the loading parameter J as the resistance R are known. As an example fracture ex-

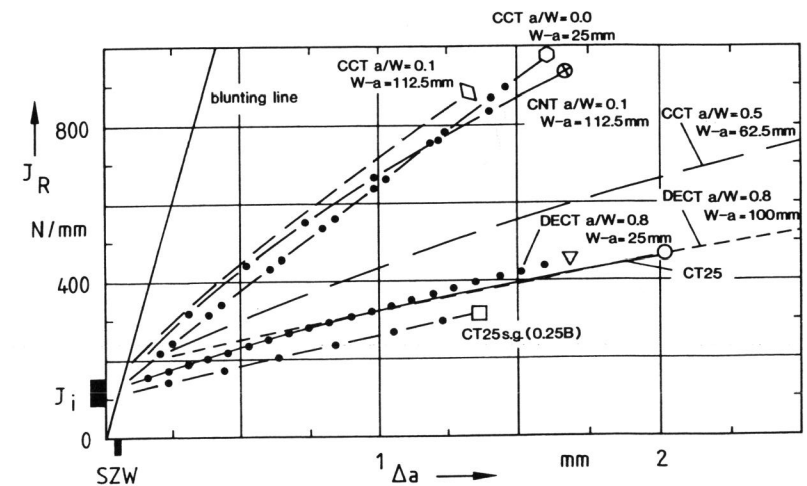


Fig. 13. J_R -Curves for Axial Through-the-Thickness Cracks in a Cylindrical Vessel ($\phi = 1.5 \text{ m}$) and Three Different Types of Specimens; Steel Ste 460 at $25 \pm 2^\circ\text{C}$. (Aurich et al. 1986).

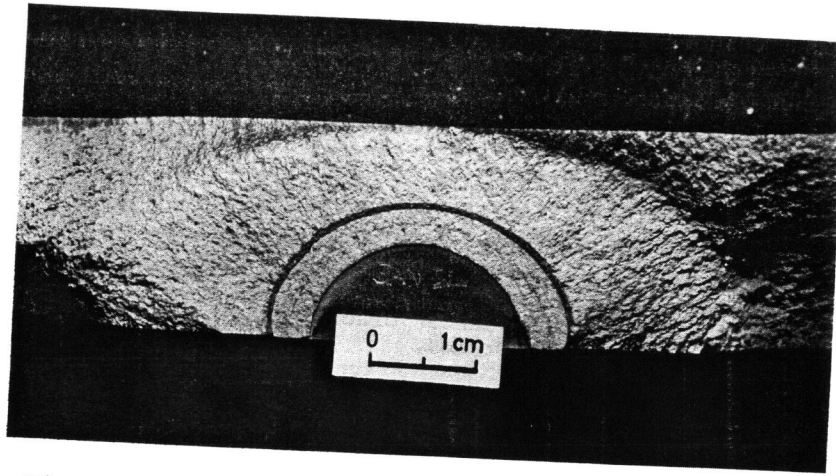


Fig. 14. Stable Growth of a Surface Crack in a Plate of X CrMoV 12 1. (Klemm et al. 1988).

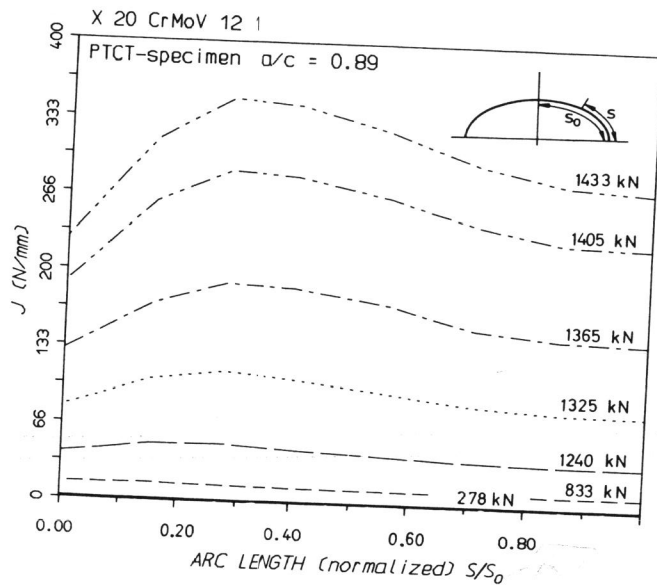


Fig. 15. J-Distribution at Several Load Steps Along the Contour of a Surface Crack ($a/c = 0.89$, $a/t = 0.6$) in a Plate Under Remote Tension. (Klemm et al. 1988).

periments are considered which are carried out in plates (900 mm x 120 mm x 20 mm) of the steel X 20 CrMoV 12 1 at room temperature. The original surface crack obtained by fatigue has been extended by stable crack growth when monotonic load was applied until the loading process was interrupted. The resulting stable crack growth surrounding the contour of the surface crack is shown as a dark zone on the fracture surface in Fig. 14. In order to predict the amount of stable growth in a quantitative manner the same procedure discussed before has been applied. The J-distributions at several load steps along the contour of this surface crack with the dimensions $a/c = 0.89$ and $a/t = 0.6$ in a plate under remote tension has been computed (Fig. 15) as well as the constraint distribution $\sigma_m / \sigma_v = h(r = 0.3 \text{ mm}, s)$ on the ligament along the crack contour (Fig. 16). Since the local distribution of the resistance is unknown it can be constructed by determining the same way as reported in Fig. 12 the linearized curve of $\Delta J / \Delta a$ in dependence of the parameter h_m for this material. After constructing the local resistance curves and inserting the related local J-values according to Fig. 15 finally the local variation of the crack extension Δa can be estimated. Although this procedure is based on a series of simplifying assumptions the resulting variation of the local crack extension $\Delta a(s)$ is in excellent agreement with the experimentally determined (Fig. 17).

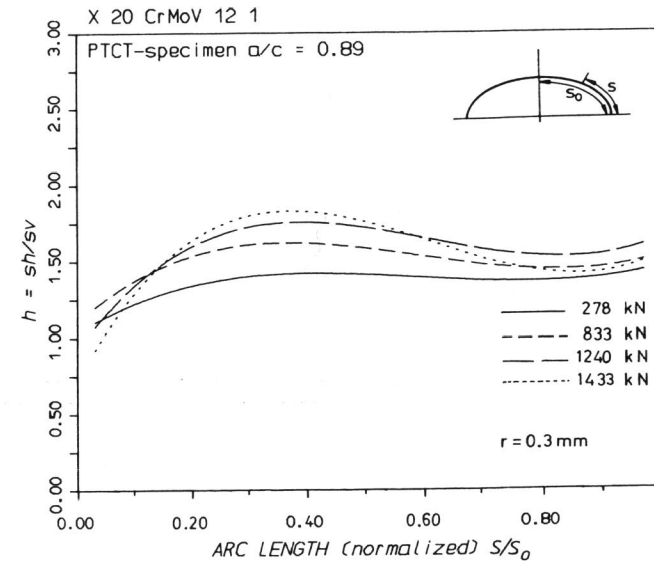


Fig. 16. $\sigma_m / \sigma_v = h(s)$ at the Distance $r = 0.3 \text{ mm}$ Along the Contour of the Same Surface Crack. (Klemm et al. 1988.)

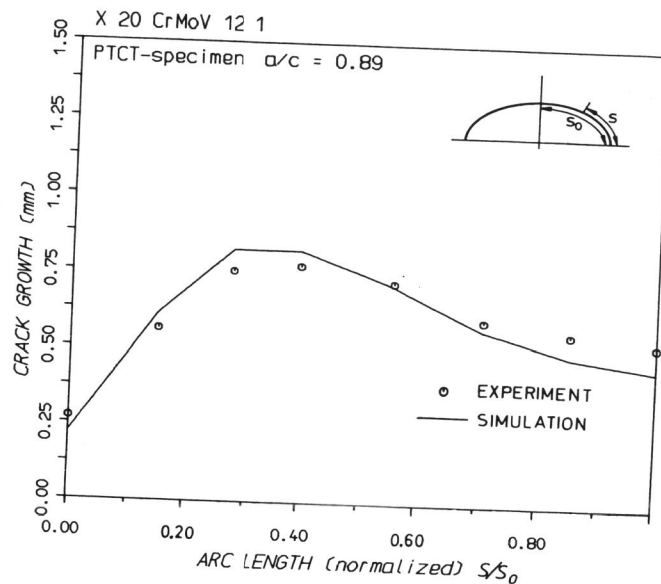


Fig. 17. Comparison of the Local Crack Extension Constructed and Experimentally Determined for the Same Surface Crack Configuration. (Klemm et al. 1988.)

It is promising that results from other authors (Brocks et al.) (s. also discussion in Aurich and Sommer) lead to the same principal results even under conditions where the maximum of the distribution $J(s)$ does not match the maximum of $\Delta a(s)$ as shown for an outer surface crack ($a/s = .22$, $a/t = .51$) in axial direction of a vessel ($\varnothing = 1.5$ m, $t = 40$ mm).

3. CONCLUSIONS

The basis for the assessment of the integrity of components and structures has been strengthened during the past years by using refined methods of EPFM. Furthermore the transferability of results obtained from small specimens to components under actual service conditions has been extremely improved including the prediction of growth characteristics of cracks. It has been demonstrated for the selected example of a surface crack extending in a stable manner that for the prediction of the local crack growth Δa not only the variation of the loading parameter $J(s)$ along the crack contour has to be known, but also the variation of the parameter of multiaxiality (σ_m / σ_v)(s).

4. REFERENCES

- Aurich, D., K. Wobst, H. Krafka (1986). J_R -Curves of Wide Plates and CT 25 Specimens; Comparison of the Results of a Pressure Vessel, 13. MPA-Seminar, Stuttgart, 46.1 - 46.20.
- Aurich, D., E. Sommer (1988). The Effect of Constraint on Elastic-Plastic Fracture. Steel Research 9, 358-367.
- ASTM Standards (1986), Philadelphia, Part 31.
- ASTM E 813-82, Determination of J_{IC} , A Measure of Fracture Toughness. Annual Book of ASTM.
- BAM-Forschungsbericht (1987). Analyse und Weiterentwicklung bruchmechanischer Versagenskonzepte auf der Grundlage von Forschungsergebnissen auf dem Gebiet der Komponentensicherheit, Teilvorhaben: Werkstoffmechanik, BAM, Berlin.
- Bathe, K.H. (1980). Adina, a Finite Element Programm for Automatic Dynamic Incremental Nonlinear Analysis. Report 82 448-1, Massachusetts Institute of Technology, Cambridge, MA, USA.
- Blauel, J.G., L. Hodulak, T. Hollstein, B. Voss (1984). Material Characterization by J_R -Curves of a 20 MnMoNi 55 Forging. Int. J. Pres.Ves. & Piping 17, 139-162.
- Blauel, J.G., B. Voss (1986). Characterization of Ductile Material Behaviour by J_R -Curves. ECF 6 Fracture Control of Engineering Structures, Vol. 1, Amsterdam.
- Brocks, W. and H.-D. Noack (1987). Elastic-plastic FEM-Analysis of an Inner Surface Flaw in a Pressure Vessel. 9 SMiRT, Lausanne, /G4/3.
- Brocks, W., H. Krafka, W. Müller, K. Wobst (1988). Experimental and Numerical Investigations of Stable Crack Growth of Axial Surface Flaws in a Pressure Vessel. Technischer Fachbericht, BAM, Berlin.
- Brocks, W., G. Künecke, H.-D. Noack, H. Veith (1987). On the Transferability of Fracture Mechanics Parameters from Specimens to Structures Using FEM. 13. MPA-Seminar, Stuttgart.
- Brocks, W. and H.-D. Noack (1987). Elastic-Plastic FEM Analysis of an Inner Surface Flaw in a Pressure Vessel. 9th Conference on Structural Mechanics in Reactor Technology, Lausanne, Vol. G, paper 4/3, 1-7.
- Brocks, W., H. Krafka, W. Müller and K. Wobst. Experimental and Numerical Investigations of Stable Crack Growth of Axial Surface Flaws in a Pressure Vessel. To be published in Proceedings of 6th Int. Conf. on Pressure Vessel Technology
- Clausmeyer, H. (1969). Kritischer Spannungszustand und Trennbruch unter mechachsiger Beanspruchung. Konstruktion, 21, 2 52-59.
- Hodulak, L., H. Kordisch, S. Kunzelmann and E. Sommer (1978). Influence of the Load Level on the Development of Part-Through Cracks. Int. J. Fracture, 14, R35-R38.

- Hodulak, L., H. Kordisch, S. Kunzelmann and E. Sommer (1977). Bruchverhalten von teilweise durchgehenden Rissen. IWM-Bericht V1/77, Freiburg, 1-99.
- IWM-CRACK, Subroutine-package for Crack Problems, 1988, Fraunhofer-Institut für Werkstoffmechanik, Freiburg.
- Klemm, W., D. Memhard and W. Schmitt (1988). Experimental and Numerical Investigation of Surface Cracks in Plates and Pipes. IAEA Specialists' Meeting on Large Scale Testing, Stuttgart.
- Kordisch, H. and E. Sommer (1986). 19th National Symposium on Fracture Mechanics, San Antonio, Texas, USA, 30.1-30.24.
- Kordisch, H., E. Sommer and W. Schmitt (1987). The Influence of Triaxiality on Stable crack Growth. 13. MPA-Seminar, Stuttgart, 7.1-7.13.
- Loss, F.J., B.J. Menke, R.A. Gray, Jr. and J.R. Hawthorn (1979). J_R -Curve Characterization of Irradiated Nuclear Pressure Vessel Steels. Washington University, Proceedings of US NRC CSNI Specialists' Meeting on Plastic Tearing Instability, St. Louis, MO, USA.
- McGowan, J.J. (ed.) (1980). A Critical Evaluation of Numerical Solutions of the "Benchmark" Surface Flaw Problem, SESA.
- Milne, I., R.A. Ainsworth, A.R. Dowling and A.T. Stewart (1986). Assessment of the Integrity of Structures Containing Defects, R/H/R6 - Rev. 3.
- Newman, J.C. Jr. (1979). A Review and Assessment of the Stress-Intensity Factors for Surface Cracks, Part-Through Crack Life Prediction, ASTM 687 (J.B. Chang, ed.), 16-42.
- Roos, E., U. Eisele, H. Silcher and D. Kießling (1987). Ermittlung von Reißwiderstandskurven auf der Basis des J-Integrals an Großproben. 13. MPA-Seminar, Stuttgart, 6.1-6.25.
- Roos, E., U. Eisele, H. Silcher and F. Spaeth (1986). Einfluß der Werkstoffzähigkeit und des Spannungszustandes auf das Versagensverhalten von Großproben. 12. MPA-Seminar, Stuttgart.
- Schmitt, W. (1986). Three-Dimensional Finite Element Simulation of Post Yield Fracture Experiments. In: Computational Fracture Mechanics - Nonlinear and 3D Problems, PVP-Vol 85, AMD-Vol. 61, 119-131.
- Sommer, E. (1984). Bruchmechanische Bewertung von Oberflächenrissen, WFT Bd. 1, Springer/Berlin/Heidelberg/New York/Tokyo.
- Sommer, E., L. Hodulak and H. Kordisch (1977). Growth Characteristics of Part-Through Cracks in Thick-Walled Plates and Tubes, Transactions of the ASME, J. Pressure Vessel Technology, 106-111.
- Swedlow, J.L. (ed.), (1972). The Surface Crack: Physical Problems and Computational Solutions, ASME.